Glucose-Responsive Nanoparticles for Rapid and Extended Self-Regulated Insulin Delivery

As Published: 10.1021/ACSNANO.9B06395

Publisher: American Chemical Society (ACS)

Persistent URL: https://hdl.handle.net/1721.1/136582

Version: Final published version: final published article, as it appeared in a journal, conference proceedings, or other formally published context

ACS NANO

Cite This: ACS Nano 2020, 14, 488–497

www.acsnano.org

ARTICLE

Glucose-Responsive Nanoparticles for Rapid and Extended Self-Regulated Insulin Delivery

Lisa R. Volpatti,[†,‡] Morgan A. Matranga,[†] Abel B. Cortinas,[†,‡] Derfogail Delcassian,[‡,§,⊥] Kevin B. Daniel,[‡] Robert Langer,[†,‡,§,▽] and Daniel G. Anderson*[,†,‡,§,▽]

[†]Department of Chemical Engineering, Massachusetts Institute of Technology, Cambridge, Massachusetts 02139, United States

[‡]David H. Koch Institute for Integrative Cancer Research, Massachusetts Institute of Technology, Cambridge, Massachusetts 02139, United States

[§]Department of Anesthesiology, Boston Children's Hospital, Boston, Massachusetts 02115, United States

[⊥]Division of Regenerative Medicine and Cellular Therapies, School of Pharmacy, University of Nottingham, Nottingham, NG7 2RD United Kingdom

[▽]Harvard–Massachusetts Institute of Technology Division of Health Sciences and Technology, Institute for Medical Engineering and Science, Massachusetts Institute of Technology, Cambridge, Massachusetts 02139, United States

Supporting Information

ABSTRACT: **To mimic native insulin activity, materials have been developed that encapsulate insulin, glucose oxidase, and catalase for glucose-responsive insulin delivery. A major challenge, however, has been achieving the desired kinetics of both rapid and extended release. Here, we tune insulin release profiles from polymeric nanoparticles by altering the degree of modification of acid-degradable, acetalated-dextran polymers. Nanoparticles synthesized from dextran with a high acyclic acetal content (94% of residues) show rapid release kinetics, while nanoparticles from dextran with a high cyclic acetal content (71% of residues) release insulin more slowly. Thus, coformulation of these two materials affords both rapid and extended glucose-responsive insulin delivery. *In vivo* analyses using both streptozotocin-induced type 1 diabetic and healthy mouse models indicate that this delivery system has the ability to respond to glucose on a therapeutically relevant time scale. Importantly, the concentration of human insulin in mouse serum is enhanced more than 3-fold with elevated glucose levels, providing direct evidence of glucose-responsiveness in animals. We further show that a single subcutaneous injection provides 16 h of glycemic control in diabetic mice. We believe the nanoparticle formulations developed here may provide a generalized strategy for the development of glucose-responsive insulin delivery systems.**

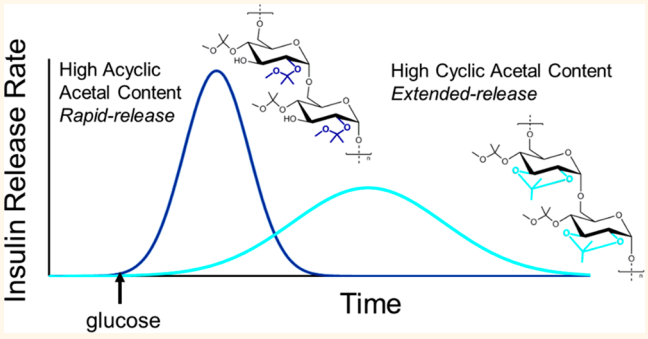

KEYWORDS: *stimuli-responsive, biomaterials, drug delivery, nanoparticles, insulin, diabetes*

Diabetes mellitus is a class of diseases in which the body either does not produce (Type 1) or is insensitive to (Type 2) insulin, resulting in poorly controlled blood glucose levels.[1] Chronic hyperglycemia often leads to severe complications including retinopathy, cardiovascular disease, kidney failure, and cancer.[1,2] These complications may be limited in both Type 1 and many Type 2 diabetic patients with intensive insulin therapy, requiring multiple daily blood glucose measurements and insulin injections.[3,4] However, intensive therapy results in decreased patient compliance[5,6] and increased risk of hypoglycemia,[7] which can cause brain damage, seizures, loss of consciousness, or death.[8,9] Current insulins on the market may be classified as rapid acting, short acting, intermediate acting, or long acting.[10−12] However, no available formulations dynamically regulate insulin release in response to glucose levels according to individual patient needs. Therefore, self-regulated delivery of insulin that mimics native insulin production in a healthy pancreas has the potential to improve diabetes therapy. Insulin pump therapy has been developed to offer continuous glucose sensing coupled with insulin infusions;[13,14] however, many challenges remain including inaccuracies of continuous glucose sensors and lags in signal feedback.[15−17]

Received: August 12, 2019
Accepted: November 25, 2019
Published: November 25, 2019

DOI: 10.1021/acsnano.9b06395
ACS Nano 2020, 14, 488–497

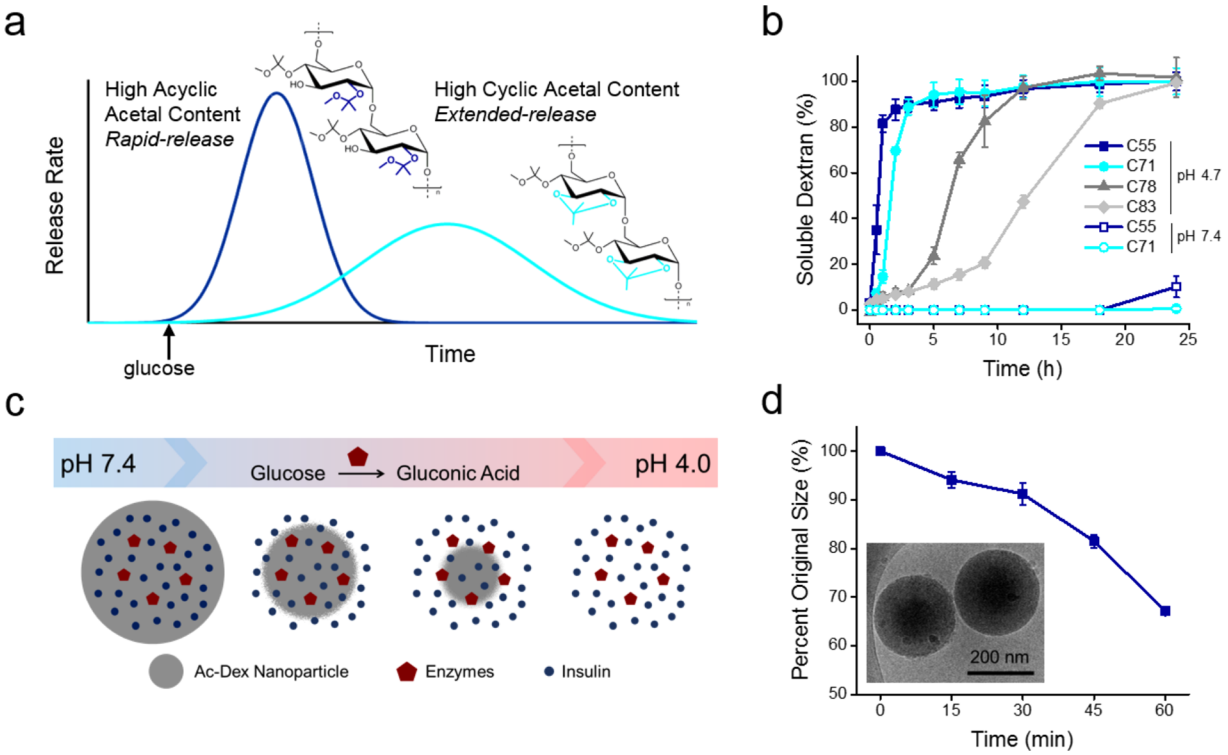

Figure 1. Desired release kinetics can be achieved by altering the properties of nanoparticles. (a) Schematic of release kinetics from rapid-release (high acyclic acetal content) and extended-release (high cyclic acetal content) Ac-dex nanoparticles. (b) Rate of degradation of Ac-dex nanoparticles by percent cyclic modification as determined by concentration of soluble dextran in the supernatant. Nanoparticles were incubated in either acetate buffer (pH 4.7) or PBS (pH 7.4) at 37 °C with agitation. (c) Schematic of glucose-responsive insulin release from acid-degradable Ac-dex nanoparticles. (d) Average relative diameter of C55NPs in acetate buffer showing reduction in size over time. Inset: cryo-transmission electron micrograph of nanoparticles at time 0.

An alternative approach is to deliver insulin with glucose-responsive biomaterials.[18] Recently, formulations have been developed that can respond to local changes in glucose with an associated change in insulin release rates.[19] Glucose detection in these systems is often mediated by the covalent attachment of a glucose-sensing moiety, namely, a boronic acid, or incorporation of the enzyme glucose oxidase (GOx).[20] GOx catalyzes the oxidation of glucose to gluconolactone which is readily hydrolyzed to gluconic acid and has been used in combination with pH-sensitive biomaterials as glucose-responsive systems.[21−23] Catalase is commonly coencapsulated with the GOx to disproportionate the reactive hydrogen peroxide byproduct and regenerate oxygen needed for the enzymatic conversion of glucose.[24−26] Since the accumulation of gluconic acid must first overcome physiological buffering effects to reduce the pH of the surrounding microenvironment, these formulations often suffer from significant delays in the glucose-responsive release of appreciable amounts of insulin. To overcome this challenge, materials have been developed that more rapidly respond to the hypoxic environment or the hydrogen peroxide generated by the enzymatic oxidation of glucose.[27−29] However, due to the rapid release of encapsulated insulin, multiple doses are required to provide glycemic control *in vivo* for up to 10 h.[27,29]

To develop a system that responds on a therapeutically relevant time scale and can afford sustained glucose-responsive insulin delivery *in vivo*, we coformulate rapid-release and prolonged-release acetalated dextran nanoparticles (Ac-dex NPs) encapsulating GOx, catalase, and insulin. We found that this combination of two types of materials is required to achieve the desired kinetics of both rapid onset and extended release of insulin. Analyses in both healthy and diabetic mouse models show direct evidence of glucose-responsiveness *in vivo*, rapid glycemic control, and prolonged normoglycemia for 16 h with a single subcutaneous injection in a diabetic mouse model.

RESULTS AND DISCUSSION

Preparation and Characterization of Ac-Dex Nanoparticles. Ac-dex is a pH-responsive polymer synthesized by reacting dextran with methoxypropene (Figure S1).[30,31] Acyclic acetal modifications are formed first which then react with neighboring hydroxyl groups to form the more stable cyclic modifications. The acetal groups are cleaved in the presence of acid to reform the native, soluble polysaccharide. Following acetal cleavage, the resultant degradation products are analyzed by ^{1}H NMR to determine the amount of each type of modification (Figure S2). Polymers with high acyclic acetal content degrade quickly while those with high cyclic acetal content have longer half-lives. A combination of nanoparticles made from these polymers can therefore provide both rapid and prolonged release kinetics (Figure 1a).

In order to develop a system with desired release kinetics, we synthesized several derivatized dextran polymers with varying degrees of modification. For reaction times between 10 and 60 min, the fraction of acyclic modifications decreases as more cyclic modifications are formed. The percentage of residues containing a single cyclic modification increases from 55% (C55) after 10 min of reaction to 83% (C83) after 60 min while the percentage of acyclic modifications decreases from

DOI: 10.1021/acsnano.9b06395
ACS Nano 2020, 14, 488−497

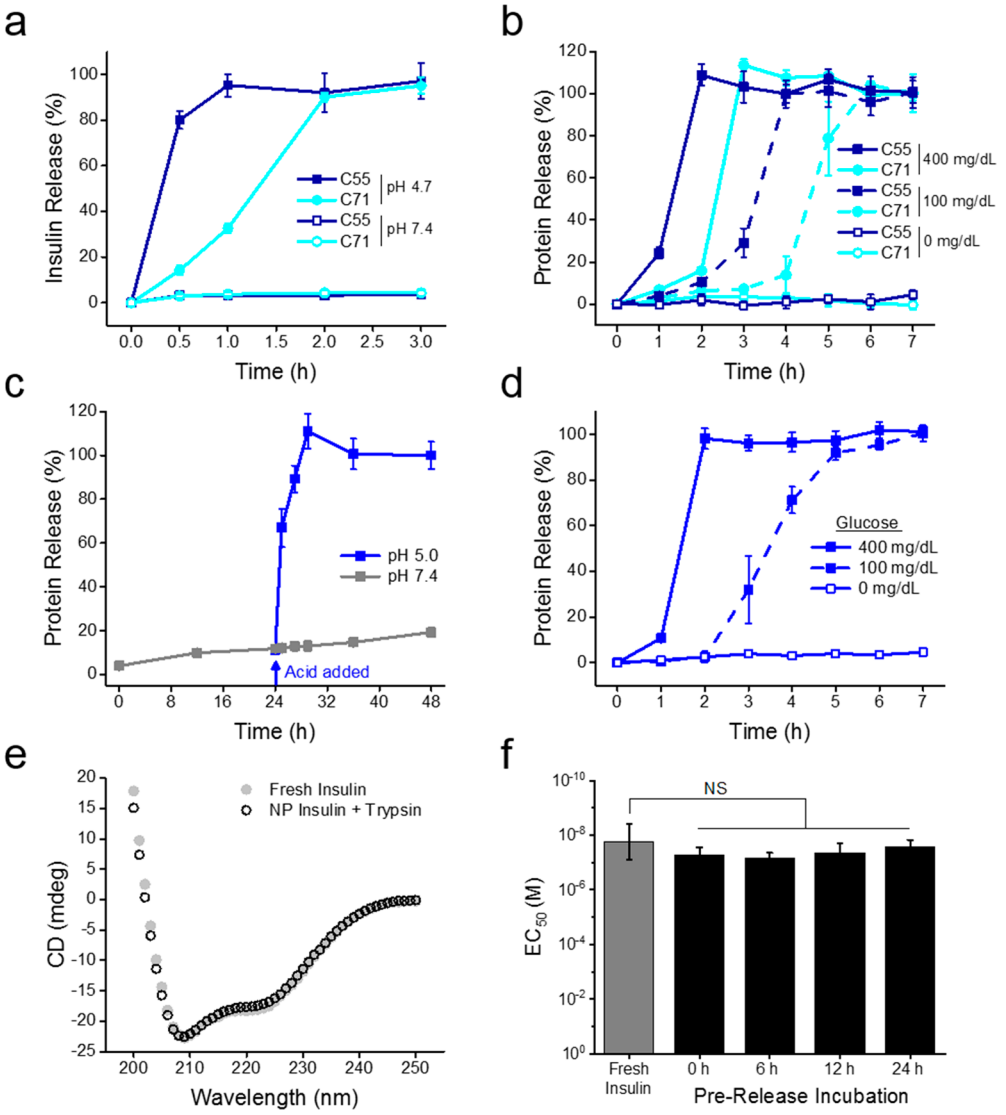

Figure 2. Coformulation of 55% and 71% (% cyclic acetalation) Ac-dex nanoparticles has fast-acting and long-acting insulin release characteristics. (a) Insulin release from C55NPs or C71NPs incubated in either acetate buffer (pH 4.7) or phosphate buffered saline (PBS, pH 7.4) at 37 °C with agitation. (b) Glucose-mediated protein release from C55NPs or C71NPs (20 mg/mL) upon incubation in PBS, PBS + 100 mg/dL glucose, or PBS + 400 mg/dL glucose at 37 °C with agitation. (c) Two regimes of protein release resulting from the addition of acid (HCl) to a mixture of C55NPs and C71NPs after 24 h of incubation. (d) Glucose-mediated protein release from a mixture of C55NPs and C71NPs (20 mg/mL). (e) Circular dichroism of released insulin after incubating NPs with 0.025% trypsin-EDTA for 24 h compared to unprocessed fresh insulin confirming retention of secondary structure. (f) EC_{50} determined by AKT phosphorylation of C2C12 cells exposed to fresh insulin or insulin released from nanoparticles after various incubation times. NS: $p > 0.05$.

94% to 83% (Figure S3). To probe the kinetics of acetal cleavage, nanoparticles with a consistent diameter (252 ± 25 nm, Figure S4a) were synthesized from a range of polymers and incubated in either acetate buffer (pH 4.7) or phosphate buffered saline (PBS, pH 7.4) at 37 °C with agitation. The amount of soluble dextran in the supernatant was measured over time to represent polymer degradation. Nanoparticles synthesized from the least modified polymer (C55NPs) were >80% degraded within the first hour, while those from polymers with an increasing percentage of modifications were more stable in acidic solution (Figure 1b). Notably, nanoparticles from the two least modified polymers showed minimal degradation upon incubation at pH 7.4 for 24 h (Figure 1b).

We next synthesized NPs (274 ± 22 nm, Figure S4b) encapsulating insulin, GOx, and catalase. GOx converts glucose to gluconolactone which is rapidly hydrolyzed into gluconic acid and reduces the pH of the microenvironment when glucose levels are high. The acetal groups of the modified dextran are subsequently cleaved, solubilizing the NPs and releasing the encapsulated insulin on demand (Figure 1c). Thus, locally regulating the pH near the NPs allows for the controlled release of insulin. To better understand the process of degradation, C55NPs were exposed to acidic solution, and their size was monitored by dynamic light scattering (DLS) over time (Figure S4c). The NPs reduced in size over the first hour reaching 67% of their original diameter before becoming undetectable by DLS (Figure 1d), suggesting that they degrade at least partially by surface erosion. Cryo-transmission electron micrographs (TEM) show spherical NPs with diameters consistent with DLS measurements at time 0 (inset, Figure 1d; Figure S5).

DOI: 10.1021/acsnano.9b06395
ACS Nano 2020, 14, 488−497

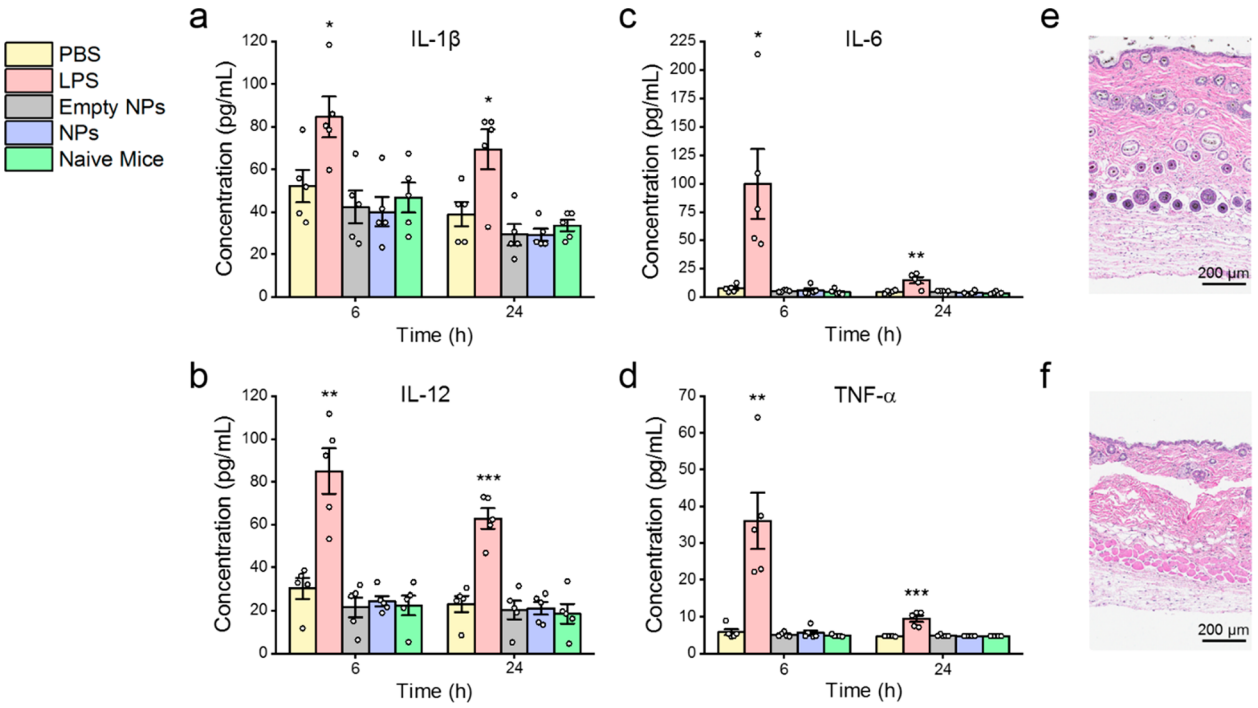

Figure 3. NP-treated mice show limited systemic pro-inflammatory cytokine response at 6 and 24 h with no prolonged local inflammatory response at 28 d according to histological analysis. Serum concentration of pro-inflammatory cytokines at 6 and 24 h following administration of PBS, 2 mg/kg lipopolysaccharide (LPS), 5 mg/kg empty NPs, or 5 mg/kg NPs encapsulating insulin and enzymes in addition to naïve mice. Analyzed cytokines include (a) IL-1*β*, (b) IL-12, (c) IL-6, and (d) TNF-*α*. Values below the standard curve are reported as less than or equal to the limit of detection of the ELISA. Data represent mean ± standard error of the mean; *N* = 5. Statistical significance is indicated by **p* < 0.05, ***p* < 0.01, and ****p* < 0.001 in comparison to PBS. H&E-stained histological images of 5 mm skin biopsies surrounding the injection site of (e) 5 mg/kg empty NPs or (f) PBS after 28 d. Representative images of five biological replicates.

The insulin loading of the C55NPs is 8.3% by mass, nearly double the amount in the C71NPs and over 6 times that in the C78NPs, which suggests that the insulin loading capacity decreases exponentially with acetalation reaction time (Figure S6a). The C55NPs contain ∼1 U GOx/mg NP, and the loading of GOx similarly decreases with percent modification (Figure S6b). The increased hydrophobicity of highly modified dextran may limit the amount of total protein loading. Thus, by varying the percent modification of the dextran, we can systematically alter the material properties to tune both the release profile and the protein loading efficiency.

Insulin Release Kinetics. To determine the kinetics of insulin release, protein-encapsulated NPs were incubated in either acetate buffer or PBS (20 mg/mL). The resultant release profiles closely follow the degradation profiles for both the C55NPs and the C71NPs (Figure 2a). The release kinetics were then studied in response to elevated (400 mg/dL) or physiological (100 mg/dL) glucose concentrations. The C55NPs show a rapid response to elevated glucose levels with virtually all insulin released after 2 h; however, they are completely degraded under physiological glucose concentrations after 4 h of incubation (Figure 2b). The C71NPs, on the other hand, have a delayed onset of release (after 2 h) with a prolonged release of insulin under lower glucose conditions (up to 6 h, Figure 2b). Based on these results, we hypothesized that a mixture of NPs could provide fast- and long-acting delivery options.

A coformulation containing equal parts by mass of C55NPs (rapid-release) and C71NPs (extended-release) shows two regimes of release in response to an acidic environment (Figure 2c). The same formulation affords a rapid onset of release in elevated glucose conditions with a more prolonged release under physiological concentrations of glucose (Figure 2d). The pH profiles are similar for the C55NPs alone, the C71NPs alone, or a mixture of the two (Figure S7). In high glucose conditions, a period of ∼2 h is required to overcome the buffering effects of the solution and decrease the pH below 5 accounting for the delayed onset of insulin release. In low glucose conditions, the pH reaches 5 after ∼4 h. Therefore, the differences in release kinetics may be attributed to the prolonged degradation of the more highly modified polymeric nanoparticles. At a lower concentration of NPs (10 mg/mL), there is a greater distinction in the onset of insulin release across a range of glucose concentrations (Figure S8a). Furthermore, insulin is released in less than an hour when NPs are first incubated in physiological glucose conditions before being exposed to elevated glucose (Figure S8b).

Activity and Biocompatibility. After analyzing the release kinetics in response to varying glucose concentrations, we then confirmed that the released insulin retains its structure and function. Insulin-encapsulated C55NPs were incubated at 37 °C with agitation in a buffer containing trypsin (0.025%) for 24 h. Circular dichroism (CD) spectra of the released insulin show excellent agreement with those of fresh insulin (Figure 2e), confirming its protection from proteolytic degradation and retention of its characteristic *α* helix structure. To show that insulin remains bioactive after formulation and release, a cell-based assay was performed to quantify the amount of AKT phosphorylation caused by the activation of the insulin receptor. The resultant dose−response curves (Figure S9) were used to calculate the EC_{50} of the sample. No significant differences in activity are observed between fresh insulin and

DOI: 10.1021/acsnano.9b06395
ACS Nano 2020, 14, 488−497

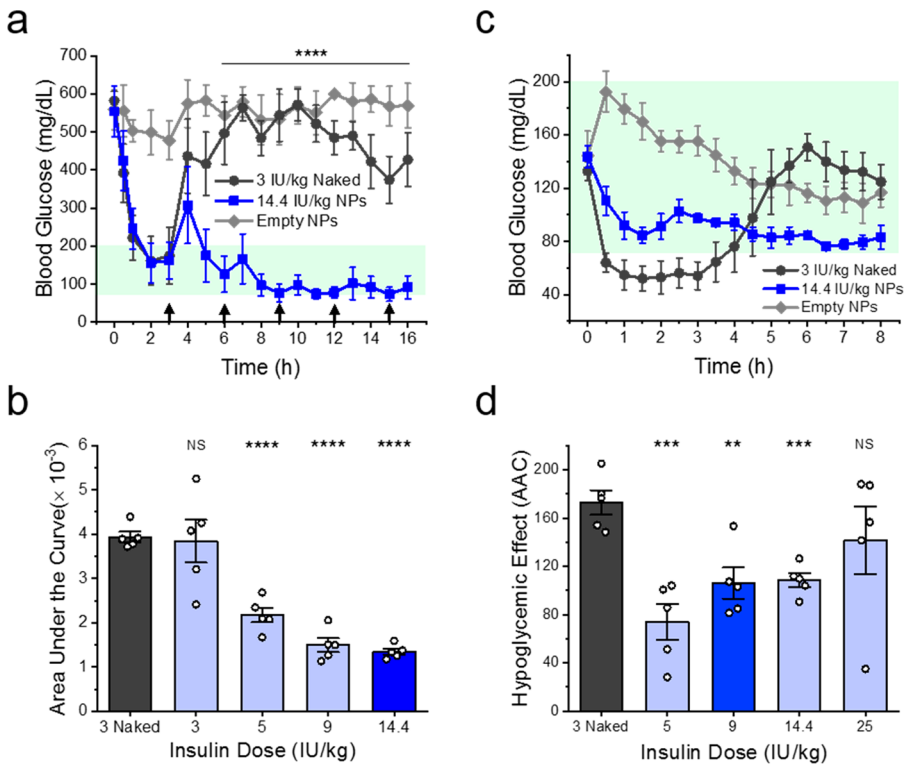

Figure 4. Doses between 5 and 14 IU/kg insulin in coformulated Ac-dex NPs show effective glycemic control in diabetic mice with limited risk of hypoglycemia in healthy mice. (a) Blood glucose levels of streptozotocin-induced type 1 diabetic mice following administration of empty NPs, 3 IU/kg naked insulin, or 14.4 IU/kg insulin in Ac-dex NPs. Arrows represent intraperitoneal glucose tolerance tests (GTTs, 1.5 g/kg) every 3 h. (b) Area under the curve for the first 9 h of (a) in addition to doses of 3, 5, and 9 IU/kg NPs. (c) Blood glucose levels of healthy mice following administration of empty NPs, 3 IU/kg naked insulin, or 14.4 IU/kg insulin in Ac-dex NPs. (d) Hypoglycemic effect calculated as the area above the curve of (c) for the first 2.5 h in addition to doses of 5, 9, and 25 IU/kg NPs. Data represent mean ± standard deviation (a, c) or standard error of the mean (b, d). Statistical significance is indicated by $^{**}p < 0.01$, $^{***}p < 0.001$, $^{****}p < 0.0001$. NS: $p > 0.05$.

insulin that has been incubated in NPs up to 24 h (Figure 2f). These results suggest that insulin is unaltered during NP processing, incubation, and release. Furthermore, NP components show minimal toxicity to these cells at the concentrations tested. To further probe cytotoxicity of intact NPs, we performed a hemolysis assay for blood compatibility (Figure S10). Hemolysis of erythrocytes was <1% for relevant doses of NPs when compared to PBS (negative control) and 1% Triton X-100 (positive control), providing further evidence of their biocompatibility.

Before determining the efficacy of the NPs *in vivo*, we tested whether they remain at the site of injection after subcutaneous (s.c.) administration in a mouse model. To study particle migration, we formulated Ac-dex NPs without proteins encapsulating a fluorescently labeled dextran (AF-680). We then s.c. injected these NPs into immunocompetent, hairless, albino SKH1E mice and quantified their fluorescence over time using an *in vivo* imaging system (IVIS; Figure S11a). Since these NPs do not contain the glucose-sensing enzyme, they are not expected to rapidly degrade and release their cargo, and the decrease in fluorescence can largely be attributed to particle migration. On day 3, the total fluorescence is on average 76.5% that of day 1, suggesting limited particle migration away from the site of injection during the time of therapeutic effect (Figure S11b).

Our Ac-dex NPs are polysaccharide based. As some types of foreign polysaccharides have been shown to cause inflammation when implanted subcutaneously,[32] we next evaluated the potential of an inflammatory response to the NPs. Systemic inflammation was assessed by measuring serum cytokine levels at 6 and 24 h post s.c. NP administration. For cytokine analysis, serum from mice treated with empty NPs or NPs containing insulin and enzymes (5 mg NPs/kg) was compared to serum from control mice treated with saline (negative control) or lipopolysaccharide (LPS, 2 mg/kg, positive control). Pro-inflammatory cytokines interleukin-1β (IL-1β), IL-6, and IL-12 and tumor necrosis factor-α (TNF-α) were significantly elevated at 6 and 24 h in mice post-treatment with the inflammatory polysaccharide LPS compared to saline-treated controls (Figure 3a–d). Granulocyte-macrophage colony-stimulating factor (GM-CSF) was significantly elevated in LPS-treated mice at 6 but not 24 h postadministration (Figure S12a). These cytokines demonstrated a greater than 1.5-fold increase in circulating systemic levels at 6 h following s.c. administration of LPS (IL-1β: 1.8-, IL-6: 19.1-, IL-12: 3.9-, TNF-α: 6.7-, and GM-CSF: 1.7-fold increase). In contrast, cytokine levels from animals treated with empty NPs or NPs containing insulin and enzymes were not significantly different from animals treated with saline, suggesting our NPs do not induce systemic inflammation (Figure 3a–d). We also analyzed levels of circulating cytokines IL-2, IL-4, IL-5, IL-10, and interferon γ (IFNγ). These cytokines were not elevated in response to LPS or administration of empty and insulin/enzyme-encapsulated NPs indicating that the Ac-dex system described is systemically noninflammatory and nonimmunogenic (Figure S12b).

DOI: 10.1021/acsnano.9b06395
ACS Nano 2020, 14, 488–497

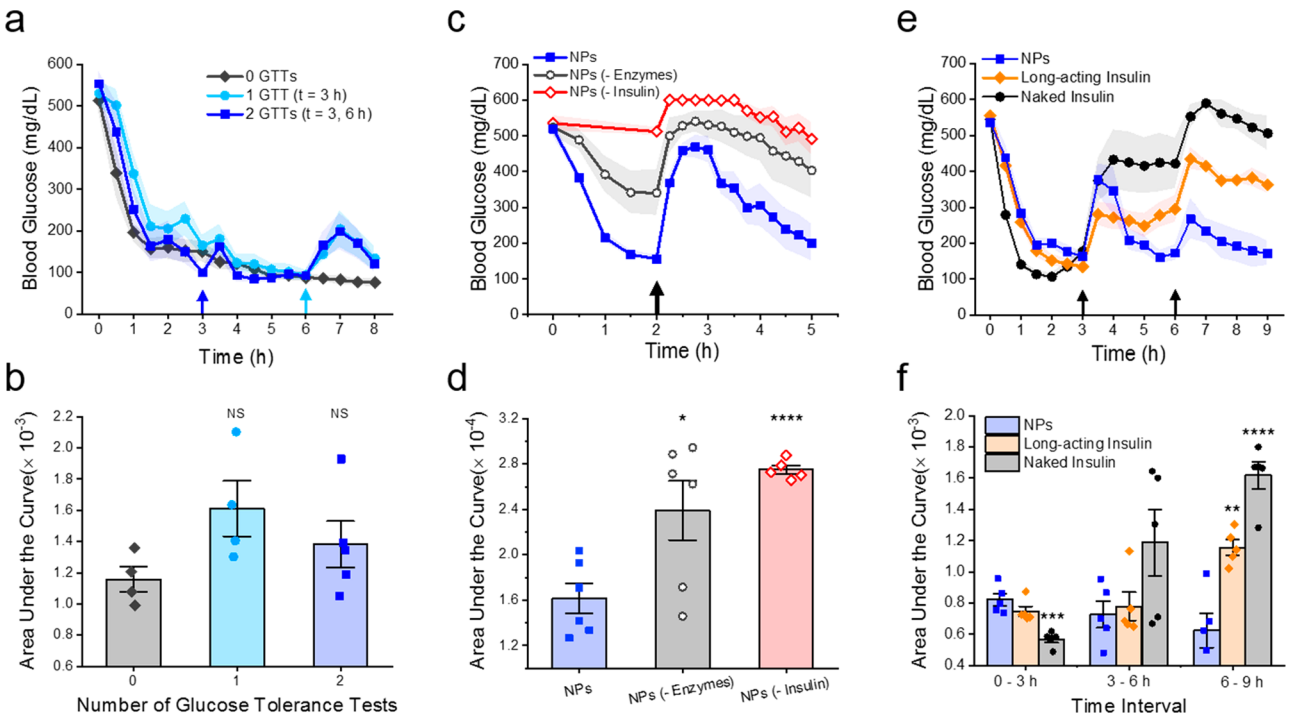

Figure 5. Glucose-responsive NPs provide similar blood glucose profiles after 0, 1, or 2 GTTs and enhance glycemic control relative to constituent components and free long-acting or native insulin. (a) Blood glucose levels of diabetic mice following administration of 9 IU/kg NPs with 0, 1 (1.5 g/kg at 3 h), or 2 GTTs (1.5 g/kg at 3 h, 2 g/kg at 6 h). (b) Area under the curve for (a). (c) Response of diabetic mice to a GTT (3 g/kg) following injection of 9 IU/kg NPs, 9 IU/kg NPs (−Enzymes), or an equivalent dose of NPs (−Insulin). (d) Area under the curve for (c). (e) Blood glucose levels of diabetic mice following administration of 5 IU/kg NPs, long-acting insulin, or naked insulin with GTTs at 3 and 6 h (1.5 g/kg). (f) Area under the curve for (e) by 3 h time interval. Shaded regions and error bars represent standard error of the mean. Statistical significance is indicated by *$p < 0.05$, **$p < 0.01$, ***$p < 0.001$, ****$p \leq 0.0001$ in comparison to NPs.

Next, local inflammation was assessed through histological analysis of skin biopsies at 1, 7, or 28 days postsubcutaneous administration of empty nanoparticles or a PBS control. The biopsies were processed for histological analysis and stained with hematoxylin and eosin (H&E). The presence of neutrophils in the H&E-stained histological images indicated that 4 of the 5 mice exhibited a local inflammatory response 1 day after NP injection (Figure S13). After 1 week, 2 of the 5 mice had few macrophages present (Figure S13). After 1 month there were no signs of inflammation in any of the 5 mice, and the H&E-stained histological images were comparable to those from the saline-treated mice (Figure 3e–f). These results are consistent with previous reports of *in vivo* biocompatibility of Ac-dex[33] and suggest that Ac-dex NPs do not cause a severe or prolonged local inflammatory response when s.c. injected in mice.

***In Vivo* Glycemic Control.** To evaluate the ability of the nanoparticles to provide glucose-responsive glycemic control *in vivo*, we employed both streptozotocin (STZ)-induced type 1 diabetic mouse and healthy mouse models. Fasted diabetic mice were subcutaneously injected with a dose of 3 IU/kg naked insulin, a coformulation of C55NPs and C71NPs at an insulin dose of 14.4 IU/kg (0.5 mg/kg), or a coformulation of empty NPs, and their blood glucose (BG) levels were monitored over time (Figure 4a). The BGs of the 14.4 IU/kg NPs group were reduced at virtually the same rate as those in the naked insulin group, indicating a rapid onset of insulin release in elevated glucose conditions *in vivo*. To test if this initial reduction in BG levels was due to nonspecific burst release, NPs were incubated for an hour *in vitro* and transferred to fresh buffer prior to injection (Figure S14a). The resultant BG profile and area under the curve (AUC) of the preincubated NPs were similar to those of directly injected NPs (Figure S14b), suggesting that this initial rapid release is specific to the *in vivo* environment.

Diabetic mice were administered an intraperitoneal glucose tolerance test (GTT, 1.5 g/kg) after 3 h to test the efficacy of the NPs in responding to a glucose challenge (Figure 4a). The mice receiving 3 IU/kg naked insulin returned to their initial hyperglycemic state directly following the GTT. In contrast, the NP group successfully regained glycemic control after an initial spike in BG levels and maintained BGs in the normoglycemic range (70–200 mg/dL) following four additional GTTs, thus providing 16 h of glycemic control with a single dose. The mice returned to hyperglycemic 2 d postinjection, indicating the potential of NPs as a once-daily treatment (Figure S15). The AUCs following 9 h and 2 GTTs show that NP doses of 5, 9, or 14.4 IU/kg insulin provide significantly enhanced glycemic control compared to 3 IU/kg naked insulin (Figure 4b, S16).

NPs were next s.c. administered to healthy mice to determine their *in vivo* response to normoglycemic conditions (Figure 4c). While mice receiving 3 IU/kg naked insulin experienced hypoglycemia, defined as having an average blood sugar concentration less than 70 mg/dL, the NP group, receiving almost 5 times the dose of insulin, remained in the normoglycemic range. The area above the curve (AAC) and below the initial BG value for the first 2.5 h is used to quantify the hypoglycemic effect. With this metric, NP doses of 5, 9, or 14.4 IU/kg insulin provide significantly reduced risk of a hypoglycemic event compared to 3 IU/kg naked insulin (Figures 4d and S17). Thus, doses between 5 and 14.4 IU/kg

DOI: 10.1021/acsnano.9b06395
ACS Nano 2020, 14, 488–497

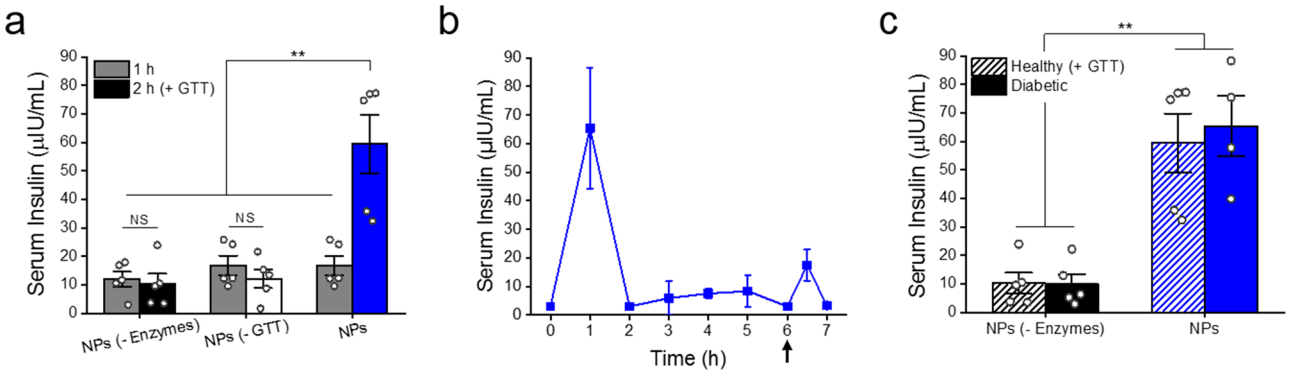

Figure 6. Coformulated Ac-dex NPs show glucose-responsive insulin release *in vivo*. (a) Serum human insulin levels of healthy mice 1 h after administration or 2 h after administration with a GTT after 1 h (3 g/kg). (b) Serum human insulin of diabetic mice following injection of NPs with a GTT at 6 h (2 g/kg). (c) Serum human insulin of healthy mice (1 h post-GTT) or diabetic mice (1 h postadministration) receiving NPs (−Enzymes) or NPs. Data represent mean ± standard error of the mean (a, c) or standard deviation (b). Values below the standard curve are reported as less than or equal to 3 μIU/mL, the limit of detection of the ELISA. Statistical significance is indicated by **$p < 0.01$. NS: $p > 0.05$.

NPs enhance glycemic control in diabetic mice and reduce the hypoglycemic effect in healthy mice compared to a single dose of 3 IU/kg naked insulin.

Since healthy mice have lower fasting BG levels than diabetic mice, they may initially experience hypoglycemia more rapidly. However, they may also respond to the insulin more rapidly by secreting counterregulatory hormones such as glucagon. Therefore, we also examined the potential for hypoglycemia in a diabetic mouse model. Mice receiving 9 IU/kg NPs were divided into three groups and administered (i) a 1.5 g/kg GTT at 3 h and a 2 g/kg GTT at 6 h, (ii) a 2 g/kg GTT at 6 h alone, or (iii) no GTTs over the 8 h study (Figure 5a). Different GTT doses were given to represent variability in glucose intake throughout the day. AUCs for groups (ii) and (iii) were not significantly different than that of group (i) (Figure 5b), and the average BGs of each group remained above 70 mg/dL for the duration of the study. These results indicate that a dose of 9 IU/kg NPs is able to attain tight glycemic control despite small differences in glucose intake and poses limited risk of hypoglycemia under these conditions in diabetic mice.

To distinguish between glucose-responsive and nonresponsive insulin release, fasted diabetic mice were administered nanoparticles containing enzymes and insulin (NPs), nanoparticles without enzymes (NPs (−Enzymes)), or nanoparticles without insulin (NPs (−Insulin)). While the *in vitro* data suggest NPs will be glucose-responsive *in vivo*, NPs (−Enzymes) are expected to slowly release insulin over time, representing basal insulin delivery. Following a 3 g/kg GTT 2 h postinjection, the average BG of all groups rises above 400 mg/dL within 30 min. After 30 min at this elevated BG level, the NP group reduces the BGs over the next 2 h and is the only group with an average BG in the normoglycemic range at the end of the 5 h study (Figure 5c). These kinetics are slightly delayed compared to the rapid initial BG reduction which may have resulted from a larger release of insulin upon initial exposure to high glucose concentrations. Nevertheless, the NPs begin to reduce the BG levels 1 h after bolus glucose administration and are ultimately able to regain glycemic control. These results suggest that all components of the nanoparticle are necessary to produce consistent glycemic control with significantly reduced AUCs (Figure 5d).

To further probe the difference between basal and glucose-responsive insulin, we next evaluated the BG levels of diabetic mice in response to equivalent doses (5 IU/kg) of NPs, a long-acting acylated analogue of insulin (commercially known as insulin detemir),[34,35] and naked insulin (Figure 5e). Compared to NPs, naked insulin initially reduces BGs more rapidly at this dose, as shown by a significantly decreased AUC for the first 2.5 h following administration (Figure 5f). However, the NP group is the only group with average BGs < 200 mg/dL following either of the 1.5 g/kg GTTs at 3 and 6 h (Figure 5e). Moreover, for the time interval between 6−9 h, the long-acting insulin and naked insulin groups both have significantly higher AUCs than the NP group (Figure 5f). Therefore, for the same dose of insulin (5 IU/kg), glucose-responsive NPs provide better extended glycemic control compared to long-acting basal or naked insulin treatments.

Glucose-Responsive Insulin Release *in Vivo*. To provide direct evidence of the translation of glucose-responsive delivery *in vivo*, we conducted time course measurements of serum human insulin concentrations in healthy and diabetic mice. Healthy mice receiving NPs (−Enzymes) or NPs experienced similar low levels of serum insulin (<20 μIU/mL) after 1 h (Figure 6a). This result corroborates our findings that the NPs do not experience a large glucose-independent burst release of insulin. At the 1 h time point, the mice were administered a GTT (3 g/kg), and the serum insulin concentration was measured after an additional hour (2 h total). Mice injected with NPs (−Enzymes) and mice that did not receive a GTT (NPs (−GTT)) had similar serum insulin levels at the 1 and 2 h time points. Conversely, there was >3-fold increase in the amount of serum insulin in the NPs group after the GTT. These results indicate that there is limited basal insulin release with a spike in release in response to glucose and both enzymes and elevated glucose concentrations are required for enhanced insulin release *in vivo*. Serum insulin of mice injected with NPs (−Insulin) were mostly below the range of detection both before and after the GTT, confirming that mouse insulin shows minimal cross reactivity with the human insulin ELISA (ALPCO) used for analysis (Figure S18).

Human insulin in diabetic mouse serum was monitored over time to quantify glucose-responsive insulin release in a diseased state. Serum insulin levels reach a maximum 1 h after injection, followed by low levels of basal serum insulin until the concentrations modestly increase immediately after a GTT at 6

DOI: 10.1021/acsnano.9b06395
ACS Nano 2020, 14, 488−497

h (Figure 6b). The relative heights of these peaks suggest that insulin release is greatest upon first exposure of the NPs to glucose, consistent with the BG reduction rates from Figure 4. Mice receiving NPs (−Enzymes) had low serum insulin concentrations for the duration of the study with no significant increase after the GTT (Figure S19a). Serum insulin concentrations are comparable in diabetic mice and healthy mice following the initial exposure of the NPs to elevated glucose levels, whether after administration or a glucose injection (Figure 6c). In both cases, serum insulin concentrations are significantly higher in the NPs group compared to the NPs (−Enzymes) group (Figures 6c and S19b). These results support the conclusion that both enzymes and hyperglycemia are required for enhanced insulin release *in vivo*.

CONCLUSION

Insulin adherence of Type 2 diabetic patients is low,[36,37] with at least 35% of patients reporting dosing omission or irregularities.[38,39] Inflexibility of scheduled insulin doses and interference with daily activities are commonly cited as contributing factors of nonadherence to prescribed insulin regimens.[39−41] A once-daily insulin injection with some flexibility of timing and dose is expected to increase patient adherence and improve quality of life of diabetic patients.[6] Furthermore, glucose-responsive insulin may have the additional therapeutic benefits of improved glycemic control by smoothing out the peaks and valleys associated with multiple self-administered doses of insulin and reduced risk of hypoglycemia corresponding to fewer visits to the emergency department.[42] While once-weekly therapies also show promise in improving patient adherence, there are additional safety risks associated with a much larger dose of insulin.

In order for a glucose-responsive delivery system to be effective, the kinetics must be rapid to quickly counteract a spike in blood sugar. Here, we report an example of fine-tuning insulin release kinetics from polymeric NPs in response to glucose by controlling the extent of polymer modification. We expect this approach to aid in the development of future glucose-responsive insulin delivery systems based on GOx. Most commercial implantable continuous glucose monitoring systems employ GOx as a sensor.[43,44] A limitation of using GOx and catalase in an injectable delivery system, however, is their potential toxicity and immune response from repeated administrations. Therefore, to take steps toward the translation of GOx-based glucose-responsive insulin delivery, methods of physically isolating the enzymes or chemically shielding them from the immune system should be further investigated.

In summary, we have developed a coformulation of rapid-release (55% cyclic modifications) and prolonged-release (71% cyclic modifications) acetalated-dextran nanoparticles encapsulating insulin and enzymes that enhances glucose-responsive delivery. Glucose-responsiveness is directly evidenced *in vivo* with an increase in serum insulin following a glucose challenge in both healthy and diabetic mice (Figure 6). A main advantage of these coformulated NPs is their ability to reduce elevated blood glucose levels in a diabetic mouse model on a time scale comparable to that of naked insulin and provide sustained delivery to afford 16 h of glycemic control after five simulated meals. In addition to providing enhanced glycemic control relative to free insulin when comparing the same dose of 5 IU/kg, these coformulated NPs also reduce the risk of hypoglycemia. Thus, the development and characterization of these coformulated, glucose-responsive nanoparticles marks an important step in the advancement of self-regulated insulin delivery.

EXPERIMENTAL SECTION

Materials/Reagents. All chemicals were obtained from Sigma-Aldrich (St. Louis, MO) and cell culture reagents from Life Technologies (Carlsbad, CA) unless otherwise noted. Recombinant human insulin (Gibco) was purchased from ThermoFisher Scientific (Waltham, MA). AlphaLISA SureFire ULTRA kits were purchased from PerkinElmer (Waltham, MA) to quantify AKT phosphorylation, and an insulin ELISA kit was purchased from ALPCO (Salem, NH) to measure serum insulin.

Nanoparticle Synthesis. Empty acetelated-dextran nanoparticles were prepared with a single-emulsion, solvent evaporation technique. Briefly, Ac-dex was dissolved in dichloromethane (DCM; 40 mg/mL) and added to a 3% poly(vinyl alcohol) (PVA) in PBS solution. This two-phase mixture was sonicated for 90 s (Q-500, QSonica, 65% amplitude) with a 1 s pulse and immediately poured into a 0.3% PVA solution. After stirring for 2 h, the mixture was centrifuged (15 min, 8000 rcf; Avanti JXN-26, Beckman Coulter) and washed twice with basic water (pH 8) before lyophilization. To form protein encapsulated nanoparticles, insulin was dissolved in carbonate buffer (pH 9.5, 100 mg/mL) with or without GOx (168.1 units/mg, 15 mg/mL) and catalase (≥20,000 units/mg, 2 mg/mL) and added to DCM containing Ac-dex (40 mg/mL). The mixture was sonicated, added to a 3% PVA solution, and sonicated a second time to form a double emulsion, which was processed in the same manner as the single-emulsion nanoparticles.

Nanoparticle Characterization. Nanoparticles were characterized by dynamic light scattering (DLS; Zetasizer Nano ZS, Malvern Instruments) and cryo-transmission electron microscopy (TEM, JEOL 2100F). Lyophilized nanoparticles were suspended in ultrapure water and filtered through 0.8 μm membrane filters before analysis by DLS or cryo-TEM. To determine degradation kinetics, nanoparticles were suspended in acetate buffer, incubated in a 37 °C shaker, and analyzed at various time points (0, 15, 30, 45, 60 min).

Acetalated-Dextran Degradation Analysis. Empty Ac-dex nanoparticles were suspended in triplicate in acetate buffer (pH 4.7) or in PBS (pH 7.4) at 5 mg/mL and incubated at 37 °C on a shaker plate. At indicated time points, aliquots were withdrawn and centrifuged. The supernatants were removed and analyzed with a microplate bicinchoninic acid assay (BCA; Pierce) according to the manufacturer's protocol using a dextran standard. The absorbance was measured at 562 nm with a plate reader (Infinite M200, Tecan).

***In Vitro* Insulin Release.** Nanoparticles containing insulin (5 mg/mL) or insulin and enzymes (10 or 20 mg/mL) were suspended in triplicate in PBS alone or with the addition of 100 mg/dL or 400 mg/dL glucose and incubated at 37 °C with agitation. At indicated time points, aliquots were withdrawn and centrifuged. The supernatants were removed and protein content was analyzed with a Coomassie Plus protein assay (Pierce) according to the manufacturer's protocol.

Insulin Structure. Secondary structural motifs were elucidated using high-performance circular dichroism (CD). Nanoparticles containing insulin (2.5 mg/mL) were incubated in a 1:10 solution of 0.25% Trypsin-EDTA:PBS at 37 °C with agitation. After 24 h, the nanoparticles were washed three times to remove the trypsin and degraded with HCl (pH 2). NaOH was used to return the pH to 7.4. This sample and fresh recombinant human insulin (200 μg/mL) were analyzed with a high-performance CD spectrometer (J-1500, JASCO Inc.) using a 0.1 cm path length cell.

***In Vitro* Activity.** The *in vitro* activity of released insulin was determined with a cellular AKT assay. To prepare for the AKT assay, C2C12 cells (American Type Culture Collection) were cultured in Dulbecco's modified Eagle medium (DMEM) containing L-glutamine, 4.5 g/L D-glucose, and 110 mg/L sodium pyruvate supplemented with 10% fetal bovine serum and 1% penicillin−streptomycin. Cells were seeded and incubated in 96-well plates at a density of 5000 cells per well. After 24 h, the cells were washed twice with serum-free DMEM and incubated for 4 h. The media was then removed, and the cells

DOI: 10.1021/acsnano.9b06395
ACS Nano 2020, 14, 488−497

were stimulated with insulin samples or controls for 30 min. The cells were then washed twice with cold Tris-buffered saline and lysed with cold Lysis Buffer (PerkinElmer) for 10 min. Concentrations of pAKT 1/2/3 (Ser473) and total AKT 1 in the cell lysates were determined with AlphaLISA SureFire ULTRA kits (PerkinElmer) according to the manufacturer's instructions. Data were analyzed using GraphPad Prism 6.0 and fit to four parameter dose−response curves to determine the EC50 of each insulin sample.

***In Vivo* Glycemic Control Studies.** All animal protocols were approved by the MIT Committee on Animal Care, and animals were cared for under supervision of MIT's Division of Comparative Medicine. The safety and efficacy of Ac-dex nanoparticles were evaluated using healthy and diabetic C57BL/6 mice (Jackson Laboratories). To induce diabetes, adult male mice were injected with a single dose of 150 mg/kg streptozotocin. Groups of at least 4 mice were fasted for 12 h and subcutaneously injected with nanoparticles, long-acting insulin, or naked insulin. Their blood glucose levels were monitored every 30 min following injection with Clarity BG1000 blood glucose meters. Glucose tolerance tests were performed by administering 1.5−3 g/kg glucose to the mice intraperitoneally. To measure serum insulin concentration, blood was collected by terminal cardiac punctures into serum gel microtubes (BD SST Microtainer). After centrifugation (5 min, 7000 rcf), serum was collected and analyzed immediately using an insulin ELISA kit (ALPCO) according to the manufacturer's instructions. Values below the standard curve are reported as less than or equal to 3 μIU/mL, the limit of detection of the ELISA.

Inflammatory Response Characterization. To quantify systemic cytokine concentration, 100 μL of blood was collected from the saphenous vein of mice following 6 h of administration of PBS, 2 mg/kg lipopolysaccharide (LPS), 5 mg/kg empty NPs, or 5 mg/kg NPs encapsulating insulin and enzymes in addition to naïve mice. Blood was collected into serum gel microtubes (BD SST Microtainer), centrifuged (5 min, 7000 rcf) and flash frozen until analysis. At 24 h, blood was collected by terminal cardiac punctures and processed similarly. Serum samples were analyzed using a mouse multiplex cytokine ELISA (Invitrogen, magnetic 10-plex: IL-1β, IL-2, IL-4, IL-5, IL-6, IL-10, IL-12, GMCSF, IFNγ, and TNF-α) run on a Luminex 200 platform. Values below the standard curve are reported as less than or equal to the limit of detection of the assay. To characterize the local inflammatory response, animals were euthanized at 1, 7, and 28 days following administration of 5 mg/kg empty NP or PBS, and skin sections surrounding the injection site were biopsied with a 5 mm biopsy punch. The tissue was fixed in 10% neutral buffered formalin overnight at room temperature. After fixation, the tissue was washed with 70% ethanol and processed for histological analysis and H&E staining. A pathologist was consulted in analysis of the samples.

Statistical Analysis. Data are expressed as mean ± standard deviation, unless otherwise indicated, and $N = 4-6$ randomly assigned mice per time point and per group. These sample sizes were chosen based on statistical power analysis and previous literature. Data were analyzed for statistical significance by unpaired, two-tailed Student's t tests.

ASSOCIATED CONTENT

Supporting Information

The Supporting Information is available free of charge at https://pubs.acs.org/doi/10.1021/acsnano.9b06395.

Additional methods and supplemental Figures S1−S19, showing polymer synthesis and characterization, nanoparticle characterization, additional *in vitro* protein release and biocompatibility studies, nanoparticle migration *in vivo* through fluorescent imaging, additional characterization of the inflammatory response, and supplemental blood glucose and serum insulin levels of both healthy and diabetic mice (PDF)

AUTHOR INFORMATION

Corresponding Author

*(D.G.A.) E-mail: dgander@mit.edu.

ORCID

Robert Langer: 0000-0003-4255-0492

Daniel G. Anderson: 0000-0003-0151-4903

Notes

The authors declare no competing financial interest.

ACKNOWLEDGMENTS

This work was supported in part by project funding provided by Sanofi, the Helmsley Charitable Trust, and the Koch Institute Support (core) Grant P30-CA14051 from the National Cancer Institute. L.R.V. was supported by a NSF Graduate Research Fellowship. D.D. was supported by a Marie Sklodowska Curie Fellowship. The authors acknowledge technical support from the Koch Institute Swanson Biotechnology Center, specifically the Animal Imaging & Preclinical Testing Core, the Histology Core, the High Throughput Screening Core, and the Nanotechnology Materials Core. The authors would like to acknowledge Dong Soo Yun for assistance with cryo-TEM and Roderick Bronson for assistance with histological analysis, in addition to Suman Bose, Kevin J. Kauffman, Owen S. Fenton, and Matthew J. Webber for helpful discussions.

REFERENCES

(1) Nathan, D. M. Long-Term Complications of Diabetes Mellitus. *N. Engl. J. Med.* **1993**, *328*, 1676−1685.

(2) Giovannucci, E.; Harlan, D. M.; Archer, M. C.; Bergenstal, R. M.; Gapstur, S. M.; Habel, L. A.; Pollak, M.; Regensteiner, J. G.; Yee, D. Diabetes and Cancer: AConsensus Report. *Ca-Cancer J. Clin.* **2010**, *60*, 207−221.

(3) The Diabetes Control and Complications Trial Research Group. The Effect of Intensive Treatment of Diabetes on the Development and Progression of Long-Term Complications in Insulin-Dependent Diabetes Mellitus. *N. Engl. J. Med.* **1993**, *329*, 977−986.

(4) Ohkubo, Y.; Kishikawa, H.; Araki, E.; Miyata, T.; Isami, S.; Motoyoshi, S.; Kojima, Y.; Furuyoshi, N.; Shichiri, M. Intensive Insulin Therapy Prevents the Progression of Diabetic Microvascular Complications in Japanese Patients with Non-Insulin-Dependent Diabetes Mellitus: A Randomized Prospective 6-Year Study. *Diabetes Res. Clin. Pract.* **1995**, *28*, 103−117.

(5) Claxton, A. J.; Cramer, J.; Pierce, C. A Systematic Review of the Associations between Dose Regimens and Medication Compliance. *Clin. Ther.* **2001**, *23*, 1296−1310.

(6) Peyrot, M.; Barnett, A.; Meneghini, L.; Schumm-Draeger, P. M. Insulin Adherence Behaviours and Barriers in the Multinational Global Attitudes of Patients and Physicians in Insulin Therapy Study. *Diabetic Med.* **2012**, *29*, 682−689.

(7) Seaquist, E. R.; Miller, M. E.; Bonds, D. E.; Feinglos, M.; Goff, D. C.; Peterson, K.; Senior, P. ACCORD Investigators. The Impact of Frequent and Unrecognized Hypoglycemia on Mortality in the ACCORD Study. *Diabetes Care* **2012**, *35*, 409−414.

(8) Cryer, P. E. Hypoglycemia, Functional Brain Failure, and Brain Death. *J. Clin. Invest.* **2007**, *117*, 868.

(9) McCoy, R. G.; Van Houten, H. K.; Ziegenfuss, J. Y.; Shah, N. D.; Wermers, R. A.; Smith, S. A. Increased Mortality of Patients with Diabetes Reporting Severe Hypoglycemia. *Diabetes Care* **2012**, *35*, 1897−1901.

(10) Siebenhofer, A. A.; Plank, J. J.; Berghold, A. A.; Narath, M. M.; Gfrerer, R. R.; Pieber, T. R. Short Acting Insulin Analogues *versus* Regular Human Insulin in Patients with Diabetes Mellitus. *Cochrane Database of Systematic Reviews*; John Wiley & Sons, Ltd.: 2004; DOI: 10.1002/14651858.CD003287.pub3.

(11) Peterson, G. E. Intermediate and Long-Acting Insulins: A Review of NPH Insulin, Insulin Glargine and Insulin Detemir. *Curr. Med. Res. Opin.* **2006**, *22*, 2613−2619.
(12) Horvath, K.; Jeitler, K.; Berghold, A.; Ebrahim, S. H.; Gratzer, T. W.; Plank, J.; Kaiser, T.; Pieber, T. R.; Siebenhofer, A. Long-Acting Insulin Analogues *versus* NPH Insulin (Human Isophane Insulin) for Type 2 Diabetes Mellitus. *Cochrane Database of Systematic Reviews*; John Wiley & Sons, Ltd.: 2007; DOI: 10.1002/14651858.CD005613.pub3.
(13) Pickup, J.; Keen, H. Continuous Subcutaneous Insulin Infusion at 25 Years. *Diabetes Care* **2002**, *25*, 593−598.
(14) Hovorka, R. Closed-Loop Insulin Delivery: From Bench to Clinical Practice. *Nat. Rev. Endocrinol.* **2011**, *7*, 385−395.
(15) Gilligan, B. J.; Shults, M. C.; Rhodes, R. K.; Updike, S. J. Evaluation of a Subcutaneous Glucose Sensor out to 3 Months in a Dog Model. *Diabetes Care* **1994**, *17*, 882−887.
(16) Wisniewski, N.; Moussy, F.; Reichert, W. Characterization of Implantable Biosensor Membrane Biofouling. *Fresenius' J. Anal. Chem.* **2000**, *366*, 611−621.
(17) Bequette, B. W. Challenges and Recent Progress in the Development of a Closed-Loop Artificial Pancreas. *Annual Rev. Control* **2012**, *36*, 255−266.
(18) Ravaine, V.; Ancla, C.; Catargi, B. Chemically Controlled Closed-Loop Insulin Delivery. *J. Controlled Release* **2008**, *132*, 2−11.
(19) Veiseh, O.; Tang, B. C.; Whitehead, K. A.; Anderson, D. G.; Langer, R. Managing Diabetes with Nanomedicine: Challenges and Opportunities. *Nat. Rev. Drug Discovery* **2015**, *14*, 45−57.
(20) Webber, M. J.; Anderson, D. G. Smart Approaches to Glucose-Responsive Drug Delivery. *J. Drug Targeting* **2015**, *23*, 651−655.
(21) Kost, J.; Horbett, T. A.; Ratner, B. D.; Singh, M. Glucose-Sensitive Membranes Containing Glucose Oxidase: Activity, Swelling, and Permeability Studies. *J. Biomed. Mater. Res.* **1985**, *19*, 1117−1133.
(22) Podual, K.; Doyle, F.; Peppas, N. Preparation and Dynamic Response of Cationic Copolymer Hydrogels Containing Glucose Oxidase. *Polymer* **2000**, *41*, 3975−3983.
(23) Wu, W.; Mitra, N.; Yan, E. C.; Zhou, S. Multifunctional Hybrid Nanogel for Integration of Optical Glucose Sensing and Self-Regulated Insulin Release at Physiological pH. *ACS Nano* **2010**, *4*, 4831−4839.
(24) Kang, S. I.; Bae, Y. H. A Sulfonamide Based Glucose-Responsive Hydrogel with Covalently Immobilized Glucose Oxidase and Catalase. *J. Controlled Release* **2003**, *86*, 115−121.
(25) Gu, Z.; Aimetti, A. A.; Wang, Q.; Dang, T. T.; Zhang, Y.; Veiseh, O.; Cheng, H.; Langer, R.; Anderson, D. G. Injectable Nano-Network for Glucose-Mediated Insulin Delivery. *ACS Nano* **2013**, *7*, 4194−4201.
(26) Gu, Z.; Dang, T. T.; Ma, M.; Tang, B. C.; Cheng, H.; Jiang, S.; Dong, Y.; Zhang, Y.; Anderson, D. G. Glucose-Responsive Microgels Integrated with Enzyme Nanocapsules for Closed-Loop Insulin Delivery. *ACS Nano* **2013**, *7*, 6758−6766.
(27) Yu, J.; Zhang, Y.; Ye, Y.; DiSanto, R.; Sun, W.; Ranson, D.; Ligler, F. S.; Buse, J. B.; Gu, Z. Microneedle-Array Patches Loaded with Hypoxia-Sensitive Vesicles Provide Fast Glucose-Responsive Insulin Delivery. *Proc. Natl. Acad. Sci. U. S. A.* **2015**, *112*, 8260−8265.
(28) Hu, X.; Yu, J.; Qian, C.; Lu, Y.; Kahkoska, A. R.; Xie, Z.; Jing, X.; Buse, J. B.; Gu, Z. H2O2-Responsive Vesicles Integrated with Transcutaneous Patches for Glucose-Mediated Insulin Delivery. *ACS Nano* **2017**, *11*, 613−620.
(29) Yu, J.; Qian, C.; Zhang, Y.; Cui, Z.; Zhu, Y.; Shen, Q.; Ligler, F. S.; Buse, J. B.; Gu, Z. Hypoxia and H2O2 Dual-Sensitive Vesicles for Enhanced Glucose-Responsive Insulin Delivery. *Nano Lett.* **2017**, *17*, 733−739.
(30) Bachelder, E. M.; Beaudette, T. T.; Broaders, K. E.; Dashe, J.; Fréchet, J. M. Acetal-Derivatized Dextran: An Acid-Responsive Biodegradable Material for Therapeutic Applications. *J. Am. Chem. Soc.* **2008**, *130*, 10494−10495.
(31) Broaders, K. E.; Cohen, J. A.; Beaudette, T. T.; Bachelder, E. M.; Fréchet, J. M. Acetalated Dextran is a Chemically and Biologically Tunable Material for Particulate Immunotherapy. *Proc. Natl. Acad. Sci. U. S. A.* **2009**, *106*, 5497−5502.
(32) Vegas, A. J.; Veiseh, O.; Doloff, J. C.; Ma, M.; Tam, H. H.; Bratlie, K.; Li, J.; Bader, A. R.; Langan, E.; Olejnik, K.; Fenton, P.; Kang, J. W.; Hollister-Locke, J.; Bochenek, M. A.; Chiu, A.; Siebert, S.; Tang, K.; Jhunjhunwala, S.; Aresta-Dasilva, S.; Dholakia, N.; et al. Combinatorial Hydrogel Library Enables Identification of Materials that Mitigate the Foreign Body Response in Primates. *Nat. Biotechnol.* **2016**, *34*, 345−345.
(33) Suarez, S.; Grover, G. N.; Braden, R. L.; Christman, K. L.; Almutairi, A. Tunable Protein Release from Acetalated Dextran Microparticles: A Platform for Delivery of Protein Therapeutics to the Heart Post-MI. *Biomacromolecules* **2013**, *14*, 3927−3935.
(34) Kurtzhals, P.; Havelund, S.; Jonassen, I.; Kiehr, B.; Larsen, U.; Ribel, U.; Markussen, J. Albumin Binding of Insulins Acylated with Fatty Acids: Characterization of the Ligand-Protein Interaction and Correlation between Binding Affinity and Timing of the Insulin Effect. *Biochem. J.* **1995**, *312*, 725−731.
(35) Havelund, S.; Plum, A.; Ribel, U.; Jonassen, I.; Vølund, A.; Markussen, J.; Kurtzhals, P. The Mechanism of Protraction of Insulin Detemir, a Long-Acting, Acylated Analog of Human Insulin. *Pharm. Res.* **2004**, *21*, 1498−1504.
(36) Cramer, J. A.; Pugh, M. J. The Influence of Insulin Use on Glycemic Control: How Well Do Adults Follow Prescriptions for Insulin? *Diabetes Care* **2005**, *28*, 78−83.
(37) Donnelly, L. A.; Morris, A. D.; Evans, J. DARTS/MEMO Collaboration. Adherence to Insulin and its Association with Glycaemic Control in Patients with Type 2 Diabetes. *QJM* **2007**, *100*, 345−350.
(38) Brod, M.; Rana, A.; Barnett, A. H. Adherence Patterns in Patients with Type 2 Diabetes on Basal Insulin Analogues: Missed, Mistimed and Reduced Doses. *Curr. Med. Res. Opin.* **2012**, *28*, 1933−1946.
(39) Peyrot, M.; Barnett, A.; Meneghini, L.; Schumm-Draeger, P. M. Factors Associated with Injection Omission/Non-Adherence in the Global Attitudes of Patients and Physicians in Insulin Therapy Study. *Diabetes, Obes. Metab.* **2012**, *14*, 1081−1087.
(40) Peyrot, M.; Rubin, R. R.; Kruger, D. F.; Travis, L. B. Correlates of Insulin Injection Omission. *Diabetes Care* **2010**, *33*, 240−245.
(41) Ross, S. A.; Tildesley, H. D.; Ashkenas, J. Barriers to Effective Insulin Treatment: The Persistence of Poor Glycemic Control in Type 2 Diabetes. *Curr. Med. Res. Opin.* **2011**, *27*, 13−20.
(42) Geller, A. I.; Shehab, N.; Lovegrove, M. C.; Kegler, S. R.; Weidenbach, K. N.; Ryan, G. J.; Budnitz, D. S. National Estimates of Insulin-Related Hypoglycemia and Errors Leading to Emergency Department Visits and Hospitalizations. *JAMA Int. Med.* **2014**, *174*, 678−686.
(43) Wang, H.-C.; Lee, A.-R. Recent Developments in Blood Glucose Sensors. *J. Food Drug Anal.* **2015**, *23*, 191−200.
(44) Vashist, S. K.; Zheng, D.; Al-Rubeaan, K.; Luong, J. H.; Sheu, F.-S. Technology behind Commercial Devices for Blood Glucose Monitoring in Diabetes Management: A Review. *Anal. Chim. Acta* **2011**, *703*, 124−136.

DOI: 10.1021/acsnano.9b06395
ACS Nano 2020, 14, 488−497